ISME

Optimization of Fuzzy Controller for an SMA-actuated Artificial Finger Robot

M.M. Kheirikhah[*]
Associate Professor

A.R. Khodayari[†]
Associate Professor

The purpose of this paper is to design and optimize an intelligent fuzzy-logic controller for a three-degree of freedom (3DOF) artificial finger with shape-memory alloy (SMA) wire actuators. The robotic finger is constructed using three SMA wires as tendons to bend each phalanx of the finger around its revolute joint and three torsion springs which return the phalanxes to their original positions. A PID controller is designed to control the rotation of each phalanx. The gains of the controller are defined and optimized using the genetic algorithm. Finally, a fuzzy PID controller is presented to improve the performance of the system. The performance of the designed controller to achieve the desired output is simulated and also tested. The rotation of each link of both prototype robot and simulated model is measured. The experimental results show that the fuzzy controller can reach the desired angle in less time and the output signal is uniform. Moreover, the simulation results indicate that the closed-loop control system of the simulated robot is in good agreement with the prototype robot.

Keywords: optimization; genetic algorithm; artificial finger prototype; fuzzy controller; simlation.

1 Introduction

The design and manufacturing of rehabilitation robots have developed in the past several years to aid the disabled and to improve their ability to control their bodies. Actuators are important components of these robot driving systems. Biomimetic robots and artificial limbs need to be light, small, and powerful actuators. Shape memory alloys (SMAs) are currently used in biomimetic robots and prosthetics because of compatibility with the human body, high power-to-weight ratio, reducing size, and simple transmission system requirements [1]. SMAs constitute a group of metallic materials with the ability to return to a predefined length or shape when they are subjected to a thermodynamic process. Transformation from the martensite crystalline structure to the austenite form creates a mechanism which changes the shape of SMAs.
The austenite phase is stable at high temperatures, whereas the martensite is stable at lower temperatures. Over the past two decades, some researchers have developed prosthetic hands which use the SMA wires as actuators.

[*]Corresponding Author, Associate Professor, Faculty of Industrial and Mechanical Engineering, Qazvin Branch, Islamic Azad University, Qazvin, Iran kheirikhah@qiau.ac.ir
[†] Associate Professor, Faculty of Mechanical Engineering, Pardis Branch, Islamic Azad University, Pardis, Iran khodayari@pardisiau.ac.ir
Receive : 2019/12/16 Accepted : 2020/03/08

A 14-degree of freedom (14DOF) dexterous robotic hand with four fingers was designed by DeLaurentis and Mavroidis [2]. This robot was actuated by SMA wires and patterned after the human anatomy. A 20 DOF five-finger hand with SMA artificial muscles was presented by Kathryn et al. [3]. Hino and Maeno [4] developed a miniature finger robot driven by SMA wires which imitated the musculoskeletal system of humans. Ashrafiuon et al. [5] proposed a planar three-link robot arm with two SMA actuators and a servomotor. O'Toole and McGrath [6] designed a 12DOF SMA-actuated artificial prosthetic hand. They embedded the SMA wires within the hand structure to improve flexibility. Bundhoo et al. [7] constructed and tested a biomimetic prosthetic hand which its actuators were accompanied by SMA wires and cables.

Also, to date, many studies have focused on controlling the SMA actuators used in artificial limbs. A new SMA position control system using a self-tuning fuzzy PID controller was introduced by Ahn and Neguyan [8]. Ahn and Kha [9] developed this PID controller obtaining its parameters from the genetic algorithm (GA). Bizdoaca et al. [10] presented a controller based on fuzzy logic for an SMA-actuated tentacle robot. A single link equipped with the SMA actuation system was controlled by Nicu-George et al. [11] using PI, PD, PID, and fuzzy logic controllers. Kheirikhah et al. [12] proposed a new SMA-actuated artificial finger robot and derived the equations of the motion of the robot. Based on the proposed robot, a three-link prototype finger was constructed using polymeric materials, and its dynamic behavior was tested by Kheirikhah et al. [13]. Kaplanoglu [14] propounded SMA-based tendon-driven actuated fingers for a prosthetic hand. The fingers had four DOFs which three of them were active and a high-speed microcontroller was used for the actuation of joint motions. Gao et al. [15] proposed a hybrid actuator combining SMA wires with a micro-DC motor for a prosthetic finger to improve reflex speed. Lange et al. [16] used an SMA actuator for robotic hands. A parallel arrangement of the SMA wires along the forearm was implemented into a hand model. An adaptive PID controller was used to control the robot motion.

Larimi et al. [17] used ANFIS to investigate the motion of a 3-DOF finger robot. They showed that the prosthetic finger prototype can follow the human finger motion. Zhao et al, [18] controlled a two-joint finger robot with pneumatic actuators using the active disturbance rejection system. Li et al. [19] proposed a position tracking control system for an artificial finger with SMA wires. The experimental results demonstrated that the presented controller has better performance than the PID controller. Controlling of an artificial finger was explored by Thoresen [20] using the neural networks. Recently, Mirzakhani et al. [21] developed a PID controller for force tracking of a 2-DOF SMA-actuated artificial finger. They used the modified Brinson' s constitutive equation to model the SMA actuators.

In this paper, based on obtained results from the simulation model and the prototype robot [12, 13], the optimal choice of parameters and system features are obtained, and a new three-link lightweight aluminum finger is constructed. In this robot, three SMA wires are used as tendons in order to adduct each phalanx of the finger, and three rotational springs are employed to return each phalanx to its original situation. According to the dynamic model of the finger, a new fuzzy PID controller is designed, implemented, and tested to control the position of the simulated model and the prototype artificial finger. The performance of the designed controller in achieving the desired output is tested, and the rotation of each link of the prototype robot and the simulated model is measured.

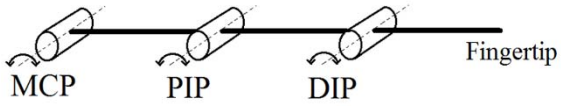

Figure 1 Schematic representation of the mechanism of the artificial finger with three DOFs

2 Modeling of the artificial finger

The human finger has three phalanxes; proximal, intermediate, and distal. Each finger has three joints: a revolute joint with two DOFs for flexion/extension and abduction/adduction in the proximal phalanx, which is named metacarpophalangeal joint (MCP), a 1DOF revolute joint for abduction/adduction in the intermediate phalanx, which is called proximal interphalangeal (PIP), and a 1DOF revolute joint for abduction/adduction in the distal phalanx, named distal interphalangeal (DIP) [13]. Fig. (1) is the schematic representation of the mechanism of the designed human finger with three DOFs, links, and joints.

In this robot, three SMA wires are used as tendons in order to adduct each phalanx of the finger. Each SMA wire is connected to the corresponding link of the robot. When the voltage is applied to each wire, because of its resistance against the applied current, the temperature of the wire rises and its length becomes shorter so that the corresponding link starts to turn. When the applied voltage is removed, the temperature of the wire is reduced and it returns to its initial length. Finally, the links are returned to their original positions by the torsional spring embedded in the joints. The motion equations of the proposed robot can be derived using the Denavit-Hartenberg method and the Lagrange equation as [12]:

$$\tau_{ij} - \tau_{si} = \sum_{j=1}^{n} D_{ij}(q)\, q_i + \sum_{k=1}^{n}\sum_{j=1}^{n} c_{kj}^{i}(q)\, q_k q_j + h_i(q) + b_i(q) \qquad i = 1,2,3 \tag{1}$$

For the *i*th link, D_{ij} is the mass matrix, c_{ikj} is the damping coefficient, h_i is related to the gravitational potential energy, and b_i is the frictional force. In this model, the friction of the joints is ignored. In addition, τ_{si} is the torque of the tension spring, and τ_{ij} is the applied torque of the SMA actuator, which can be defined as below:

$$\tau_{si} = k_i \theta_i \qquad i = 1,2,3 \tag{2}$$

$$\tau_{ij} = r_{pi}\sigma_i A_i \quad , \qquad A_i = \pi r_{wi}^2 \quad i = 1,2,3 \tag{3}$$

Where k_i is the stiffness of the torsional spring, r_{pi} is the pulley radius, σ_i is the normal stress of the wire, A_i is the cross-sectional area of the wire, and r_{wi} is the wire radius for the *i*th link. The strain rate ($\dot{\varepsilon}_i$) of the SMA wire of the *i*th link can be calculated as:

$$\dot{\varepsilon}_i = \frac{-r_{pi}\dot{\theta}_i}{l_{wi}} \qquad i = 1,2,3 \tag{4}$$

where l_{wi} is the initial length of the *i*th wire.

To model the thermodynamic behavior of the SMA wire actuators, the thermal properties of these materials, heat transfer behavior, constitutive laws, and phase transformation models must be considered. In this robot, the SMA actuators are heated by applying the electric current and are cooled by the surrounding air. Hence, the free convection heat transfer model of the wires can be defined as below [22]:

$$m_{wi} c_p \frac{dT_i}{dt} = \frac{V_i^2}{R_i} - (h_0 + h_2 T_i^2)\, A_{li}(T_i - T_\infty) \quad i = 1,2,3 \tag{5}$$

where m_{wi} is the mass, V_i is the voltage of the applied current, R_i is the electrical resistance, T_i is the temperature, and A_{li} is the surface area of the *i*th wire. Also, c_p is the specific heat, h_0 and h_2 are the heat convection coefficients, and T_∞ is the surrounding temperature.

The relationship between the stress, strain, and temperature of a material is defined by its constitutive law. There are many constitutive laws for SMAs, but the most important and applicable law is the Liang constitutive law. The Liang model is defined as [23]:

$$\dot{\sigma}_i = D\dot{\varepsilon}_i + \Theta_T \dot{T}_i + \Omega_i \dot{\xi}_i \qquad i = 1, 2, 3 \tag{6}$$

where $\dot{\sigma}$ is the stress rate, $\dot{\varepsilon}$ is the strain rate, $\dot{T}$ is the temperature rate, and $\dot{\xi}$ is the rate of change in martensite fraction of the SMA wires. Furthermore, Θ_T is the thermal expansion coefficient, D is the modulus of elasticity, and Ω_i is the coefficient of phase transformation.

The martensite fraction (ξ_i) depends on the temperature and the stress of the SMA material and is defined as [23]:

$$\xi_i = \frac{1}{2}\{cos[a_A(T_h - A_s) + b_A\sigma_i] + 1\} \qquad i = 1, 2, 3 \tag{7}$$

In this model, the coefficients a_A and b_A can be defined as below:

$$a_A = \frac{\pi}{A_f - A_s} \quad , \quad b_A = -\frac{\pi}{c_A} \tag{8}$$

where A_s and A_f are the initial and final temperatures of the austenite phase transition.

The state vector of the angles of the joints, the angular velocities of the joints, the temperature of the SMA wires, the wires stresses, and the martensite fractions can be defined as the following:

$$x = [\theta_1 \quad \theta_2 \quad \theta_3 \quad \dot{\theta}_1 \quad \dot{\theta}_2 \quad \dot{\theta}_3 \quad T_1 \quad T_2 \quad T_3 \quad \sigma_1 \quad \sigma_2 \quad \sigma_3 \quad \xi_1 \quad \xi_2 \quad \xi_3] \tag{9}$$

By substituting the time derivative of Eq. (7) and Eqs. (1) and (5) into the constitutive law, the state equations can be calculated [12]. Finally, the dynamic model of the finger with the SMA wire actuators is simulated in MATLAB®2012a (The MathWorks, Inc., Natick, MA, USA).

3 Constructing the artificial finger

As stated earlier on, based on the previous studies of the present authors [12, 13], a three-link lightweight finger was made. Fig. (2) shows the top view of the constructed artificial finger. It can be seen that the finger has three links with different lengths which are connected to a fixed part. Each link is connected to the next link by a pin. Each pin is equipped by a torsional spring to return the corresponding link to its original position. Moreover, an encoder is connected to each pin to measure the rotation of the corresponding link. All links and pins are made from aluminum while the springs are made from steel.

In this robot, three SMA wires are used as the tendons of the finger. An electric-proof guide is mounted on the bottom of each link. The SMA wires are passed along these electric-proof guides, are connected to the corresponding links, and are then returned. The two ends of the wires are connected to the fixed pins, and the current is applied to each wire. Because of the electrical resistance of the wires, their temperature rises and their length becomes shorter so the links start to turn. When the applied voltage is removed, the temperature of the wires is reduced and the wires returns to their initial length. Lastly, the links are returned to their original positions by the torsional springs. Fig. (3) displays the constructed artificial finger in its original and rotated positions.

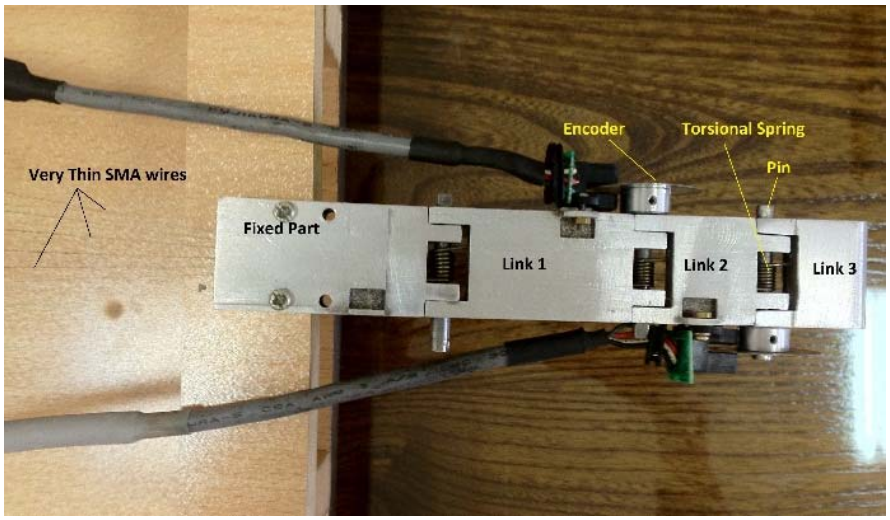

Figure 2 The constructed artificial finger viewed from above

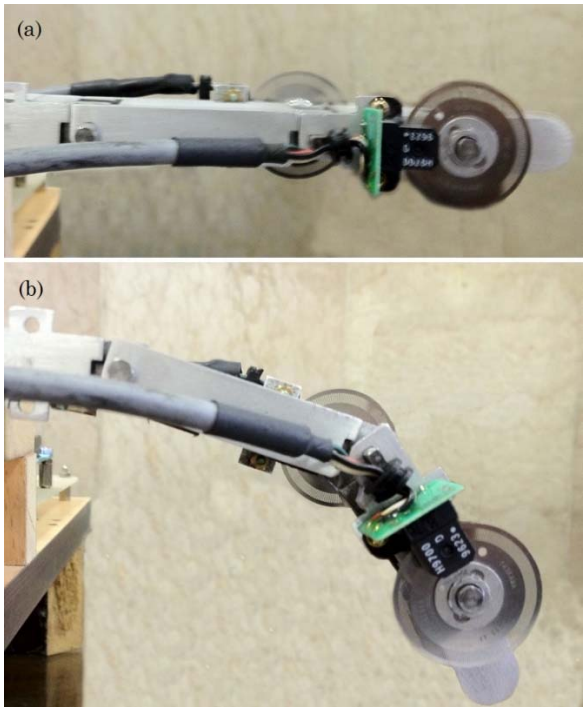

Figure 3 The artificial finger: (a) original status (b) rotated status

Table 1 The characteristics of the links and joints

Link No.	Length (mm)	Mass (kg)	Spring constant (N/m)	Pully radius (m)
1	44.8	0.011	2	0.0075
2	26.2	0.006	1.5	0.0037
3	17.7	0.004	2	0.0027

Table 2 Geometry and heat transfer model parameters of the wires

Wire	r_{wi} (mm)	l_{wi} (m)	m_{wi} (kg)	h_0	h_2	R (Ω)
1	0.187	0.38	0.1539e	70	0.001	3.08
2	0.187	0.42	0.1678e	70	0.001	3.36
3	0.187	0.44	0.1762e	70	0.001	3.52

Once the robot was constructed, its physical properties were measured. The measured properties of the joints and links of the robot are given in Table (1). These properties are also used in the simulation of the robot motion. The dynamic behavior of the robot corresponds to the thermodynamic behavior and thermal stability of the SMA actuators. The SMA wires employed in the present project have been made of nickel-titanium (NiTi) alloys produced by DYNALLOY [24]. Table (2) presents the thermal properties of the used NiTi wires [24].

In this model, the initial and final temperatures of the austenite phase transition are assumed A_s = 75 ºC and A_f = 110 ºC, respectively. Also, the specific heat of the wires is assumed to be 322 J/Kg ºC [24].

The surrounding temperature significantly affects the thermal behavior of the wires. Hence, during tests, the ambient temperature (T_∞) was kept constant at 23 ºC using an air conditioning system. Table (3) shows the parameters and coefficients used for Eqs. (7) and (8).

In the present study, to control the motion and position of the prosthetic finger, a driver board was designed and constructed for the controller. The basic function of this board is to communicate between software and hardware and to transfer, collect, and exchange the data between system parts. This board consists of 5 sections: a controlling section, an interface section, a nutrition section, a driver section for the SMA actuators, and a monitoring section. Fig. (4) illustrates the constructed driver board and its components.

The core of the controlling section contains the ATMEGA32 microcontroller. It receives the signals of the encoders from input channels and analyzes them. Subsequently, it sends the data of the encoders to the MATLAB®2012a (The MathWorks, Inc., Natick, MA, USA) and receives the control signals. Finally, it sends control commands to the drivers of the SMA wires. In the present study, the desired angles of the robot links are applied as input to the system. Then, the designed system controls the robot to achieve the desired orientation. In this system, the SMA wires act as actuators, and the encoders measure the rotation of the links.

Also, the real time measurements of the rotation angles of the links and the applied voltages are displayed in the designed controlling program. When a desired angle is defined for the PC, the designed controlling program issues the commends to the system. The data is transferred to the microcontroller by a driver circuit, and the microcontroller processes the data. Later, it creates a control pulse-width modulation (PWM) signal that is applied to each link of the artificial finger through the SMA driver. As a result, the PWM signal is converted to a proportional voltage which is applied to the SMA actuators. The interface circuit performs pre-processing on the data of the encoders and prepares them for using by the microcontroller. The microcontroller sends the data of the encoders to the computer in real time. Finally, using an interface program, the designed controller in Simulink issues the controlling commends to the links of the artificial finger.

Table 3 SMA wire constitutive and phase transformation parameters

Wire	C_A (Pa/ºc)	Initial Strain	Θ_T	Ω	D_A (Pa)	D_M (Pa)
1	10.3e6	-26.144e6	0.055e6	20.6e8	75e9	28e9
2	10.3e6	-11.004e6	0.055e6	20.6e8	75e9	28e9
3	10.3e6	-22.616e6	0.055e6	20.6e8	75e9	28e9

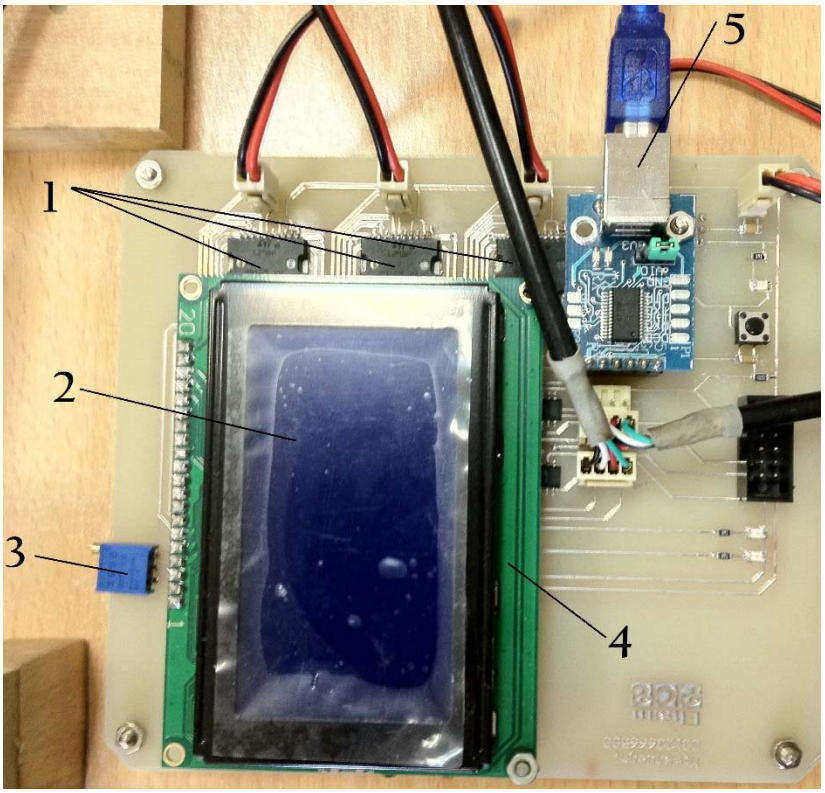

Figure 4 The driver board (1) Drivers, (2) LCD, (3) Potential meter, (4) Board consists of processor, and (5) USB to TTI transduce

4 Genetic algorithm for PID tuning

For an excellent control system design, appropriate controller parameters must be determined [25]. This process increases the stability of the system and reduces the steady-state error (SSE). In this study, a PID-fuzzy closed-loop control method is defined and used. The controlling program is expressed and simulated in MATLAB®2012a (The MathWorks, Inc., Natick, MA, USA). The block diagram of the designed controller is portrayed in Fig. (5).

To avoid using a complex control system, “gain constants” is used for the fuzzy-based controller. Also, by trial and error, further improvements in the controlling process are achieved. When the error value is large, this procedure improves the performance of the proportional action and decreases the integral action. However, the settling time is not desired. Therefore, an optimization method must be employed to define the controller gains.

The tuning of a PID controller involves selecting gains K_p, K_i, and K_d so that performance specifications are satisfied. In the current study, a GA optimization method is used for tuning the PID controllers. GA provides an adaptive searching mechanism inspired on Darwin's principle of reproduction and survival of the fittest [26]. The individuals (solutions) in a population are represented by chromosomes, each associated with a fitness value (problem evaluation). The chromosomes are subjected to an evolutionary process that takes several cycles. Some advantages of using GA are as follows: it is a global search technique, it can be applied to the optimization of ill-structured problems, and it does not require a precise mathematical formulation for the problem. Besides, GAs are robust, applicable to a number of problems, and efficient in the sense that either a suboptimal or optimal solution may be found within a reasonable length of time.

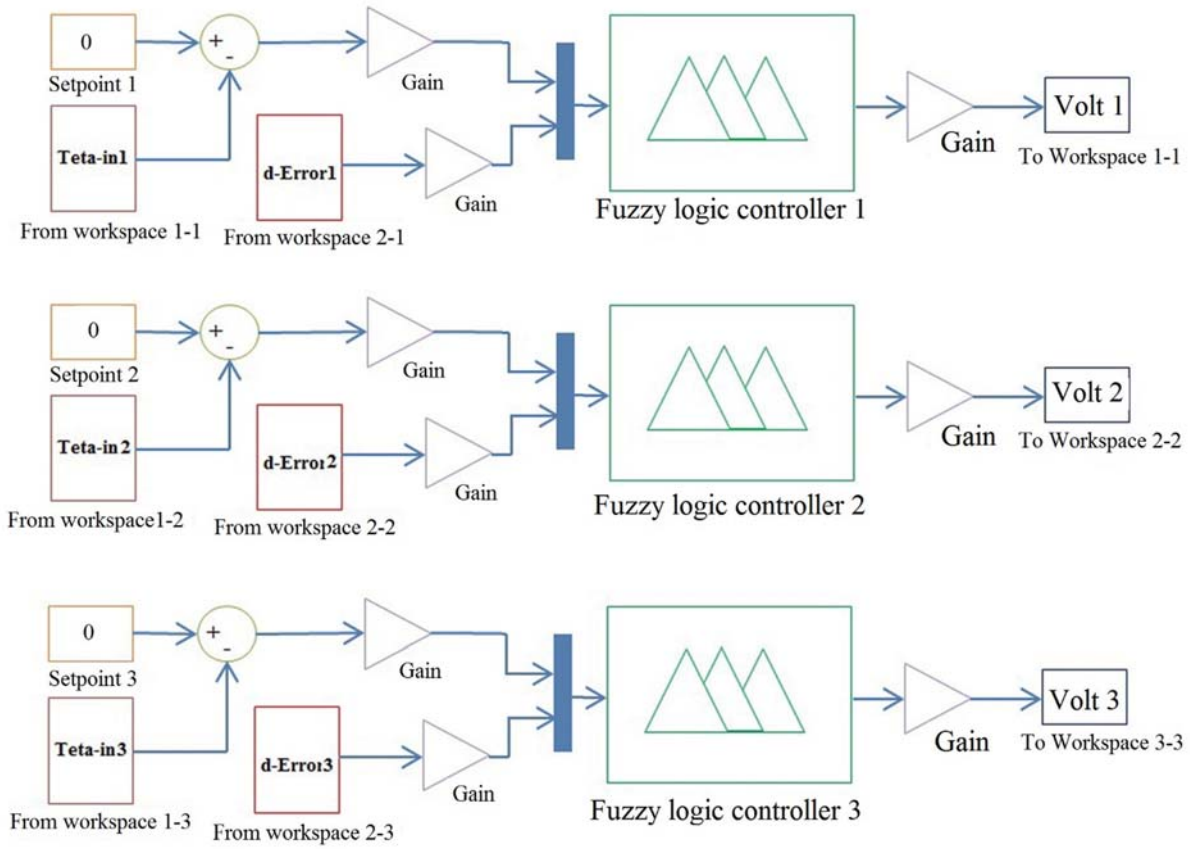

Figure 5 The block diagram of the designed PID-fuzzy controller

The implementation of the tuning procedure through GAs starts with the definition of the chromosome representation. Here, the chromosomes are formed by the three gains to be adjusted in order to achieve a satisfactory behavior. The gains K_p, K_i, and K_d are real numbers and characterize the individual to be evaluated.

The fitness function is defined as the error between the setpoint (desired output) and the system output (measured amounts of the feedback):

$$Fitness = \sum^{n} [Desired\ output - Actual\ output]^2 \quad (10)$$

The observation interval is divided up into *n* points, or samples; the error for each sample is calculated and entered into Eq. (10), which gives the sum of all errors squared as a result. The minimization of Eq. (10), performed by GA by adjusting the PID gains, will ensure that the output is as close as possible to the desired one. GA is configured as follows:

· Population: 80
· Generations: 120
· Crossover (arithmetic and one-point): 0.8
· Mutation: 0.06

The performance of the designed closed-loop PID controller in rotation control of the Link 1 (MCP) of the simulated robot was investigated. Fig. 6 demonstrates the rotation angle of this link for the two designed controllers (trial and error and GA-optimized). In this figure, the setpoint of 20 degrees is assumed. This figure shows that the output signals for both of the controllers are uniform and the time spent to achieve the desired angle and the SSE is very little. However, it is clear that the GA-optimized PID controller performs better than the other one because it has a smaller overshoot and a shorter settling time.

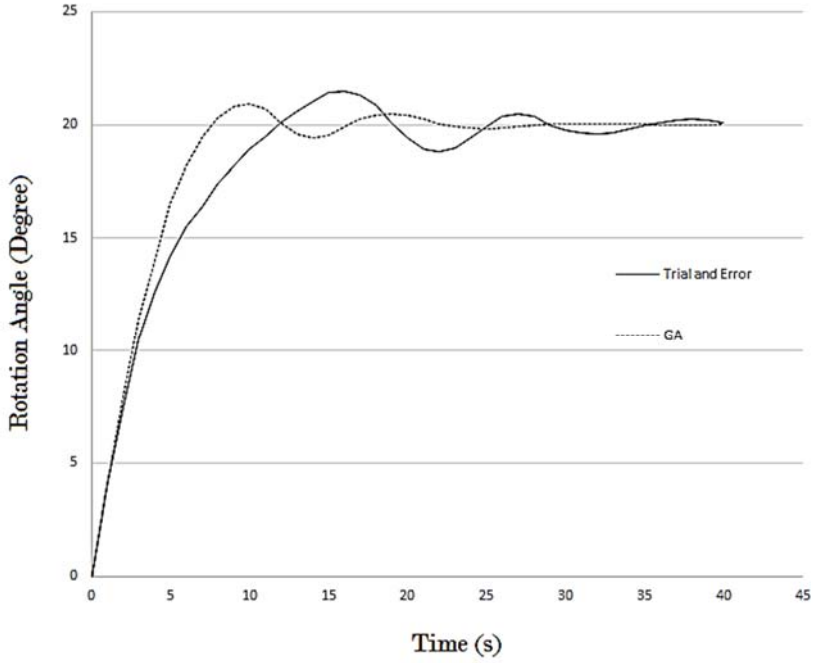

Figure 6 The rotation angle of Link 1 of the simulated robot

5 Designing a fuzzy controller system

In the designed PID-fuzzy controller, the value of the desired angles of the robot links (i.e., system input) is compared with the measured amounts of the feedback. The difference between the desired angles of the robot links and the measured one is named the position error. Then, this signal is applied as input to the fuzzy controller. For each link, the first fuzzy controller has two inputs: the error (proportional action) and the delta error (derivative action). To normalize the performance of the fuzzy controller, a constant gain is multiplied by the output. Therefore, the error which is the output of the first controller is applied as input to the second fuzzy controller. Lastly, the voltage rate of the SMA wires in obtaining the desired angle is calculated by the output of the fuzzy controller.

The structure of the designed fuzzy controller consists of some membership functions for inputs and output. This paper assumes 10 membership functions for the error (E) as {N, P1, P2, P3, P4, P5, P6, P7, P8, P9} and three membership functions for the derivative error (dE) as {N, Z, P} in each input of the fuzzy controller and nine membership functions as {V1, V2, V3, V4, V5, V6, V7, V8, V9} in the output of the fuzzy controller. Based on fuzzy control theory, these membership functions are tuned by the designed control gains and in the real situation, the domain of the variables become more expand or narrower like real values. Fig. (7) shows the membership functions of the error, the derivative error, and the output, respectively. These membership functions are defined normally.

In the present study, the rules of the controller can be expressed as follows:

The negative error means that the value of the link's angle is larger than the desired angle, and the applied voltage must be reduced.

The positive error means that the value of the link's angle is smaller than the desired angle, and the applied voltage must be increased. Table 4 shows the rules of the fuzzy controller.

In the current study, an intelligent approach is used to determine the gains of the controller. To optimize the performance of the designed fuzzy controller, a code is developed for accessing the robot behavior subjected to different inputs. The code obtains the appropriate values for the gains of the error and the delta error.

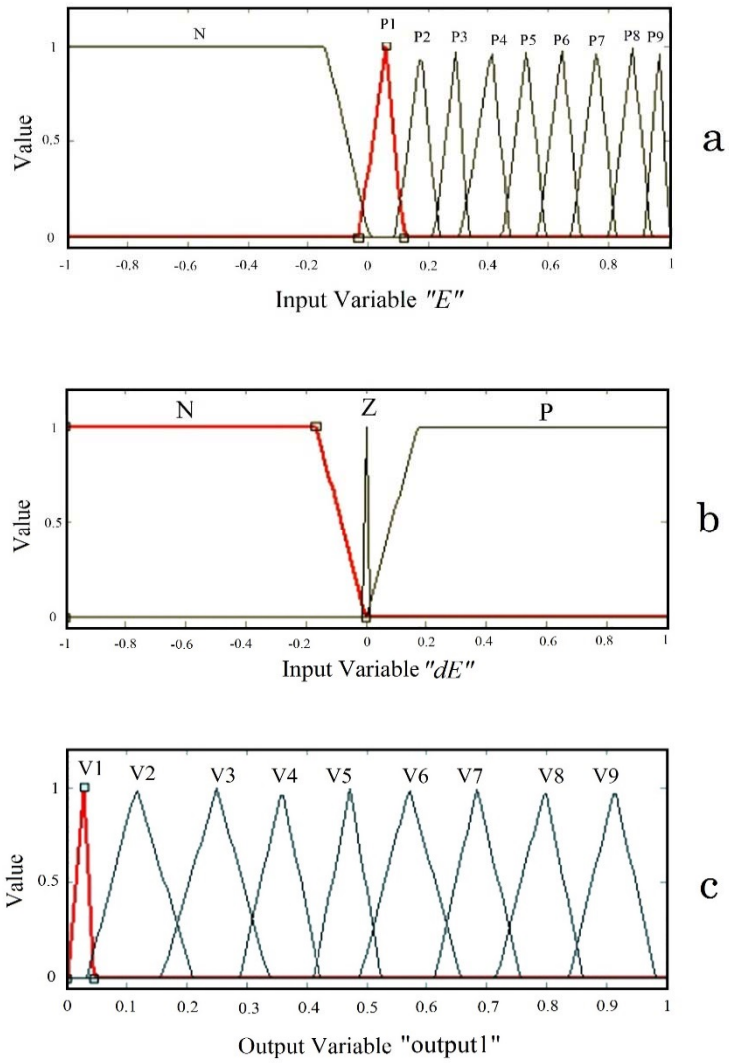

Figure 7 Membership functions for **(a)** the error **(b)** the derivative error **(c)** the output variable (V)

Table 4 Rules for the first fuzzy controller

E(t) / dE(t)	N	P1	P2	P3	P4	P5	P6	P7	P8	P9
N	V1	V1	V1	V1	V2	V2	V2	V3	V3	V3
Z	V1	V1	V2	V3	V4	V5	V6	V7	V8	V9
P	V3	V3	V3	V4	V4	V4	V5	V5	V5	V6

A gain *GEi (t)* is applied to the error before entering the fuzzy controller of each link, which is defined as below:

$$GE_i(t) = \frac{1}{setpoint\ \mathrm{i}} \qquad i = 1, 2, 3 \tag{11}$$

Also, a gain *GdEi (t)* is applied to the delta error before entering the fuzzy controller of each link, which is defined as follows:

$$GdE_i(t) = \frac{1}{(1000 \times setpoint\ \mathrm{i})} \qquad i = 1, 2, 3 \tag{12}$$

6 Results and discussion

In this section, the performance of the designed closed-loop PID-fuzzy controller in rotation control of the links of the prototype artificial finger is explored. Furthermore, to evaluate the performance of the simulated system, the results of the simulation are obtained and compared with experimental results for the same conditions.

Fig. 8 shows the rotation angle of Link 1 (MCP) of the prototype robot and the simulated robot. In this figure, the setpoint of 20 degrees is assumed. The rotation of the link is measured by its encoder for the prototype robot and is calculated via dynamic equations for the simulation model. This figure shows that the output signal is uniform and the time spent to achieve the desired angle and the SSE is very little. Additionally, the robot is not disturbed and fluctuated. Hence, the performance of the designed PID-fuzzy controller at Link 1 of the prototype robot is successful.

Fig. (9) depicts the rotation angle of Link 2 (PIP) of the prototype robot and the simulated model. For both systems, the setpoint of 18 degrees is assumed. In this figure, the uniformity of the output signal and the little time required to achieve the desired angle of Link 2 of the prototype finger confirm the successful performance of the controller. However, the system cannot achieve the exact desired output, and a little SSE remains. Fig. (10) illustrates the rotation angle of Link 3 (DIP) of the prototype robot and the simulated robot for the setpoint of 17 degrees. According to this figure, the performance of the designed PID-fuzzy controllers of the artificial finger is good. It can be seen that the steady response of the system fluctuates. It seems that this problem is due to the mechanical tolerances of the robot links, which were done in the manufacturing process of the links and their errors are integrated at the last link.

A comparison of the experimental and simulation results indicates that the closed-loop control system of the simulated robot is in good agreement with the prototype. The behavior of the prototype robot confirms the authenticity, validity, and accuracy of the simulation model. The calculated results of the all links of the simulated robot in the final position have some vibrations that are not seen in the measured results of the prototype robot. This may be because of the friction of the revolute joints which eliminates the few vibrations of the links. The performance of the fuzzy controller is good at decreasing the maximum overshoot and increasing stability. Further, the output of the designed controller is reliable and has small errors.

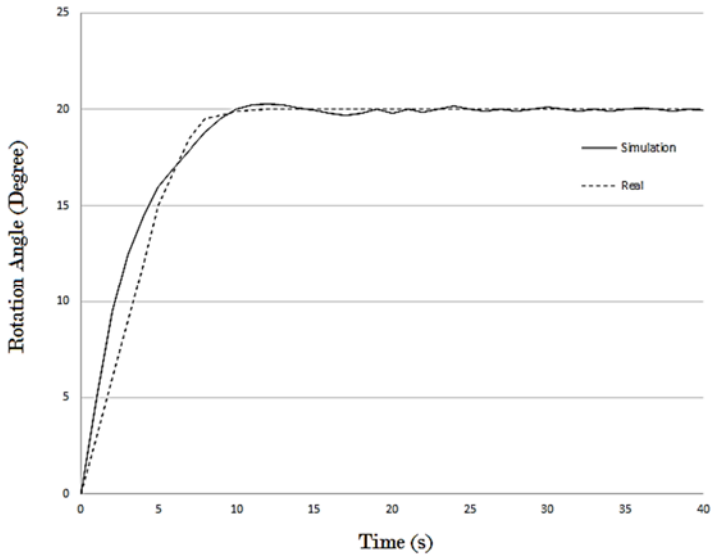

Figure 8 The rotation angle of Link 1

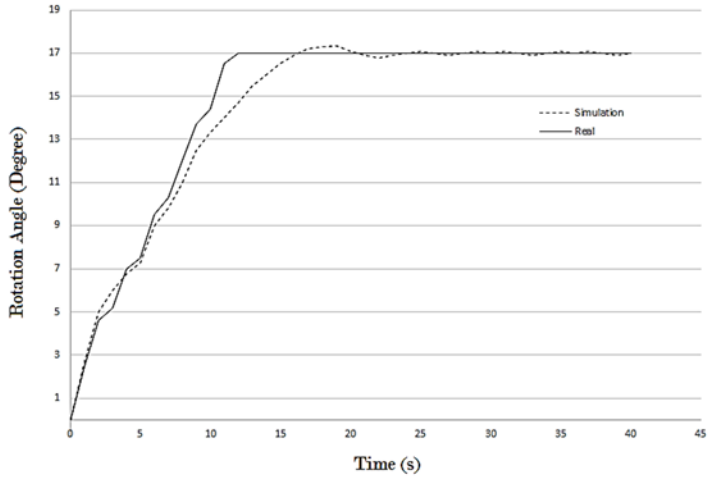

Figure 9 The rotation angle of Link 2

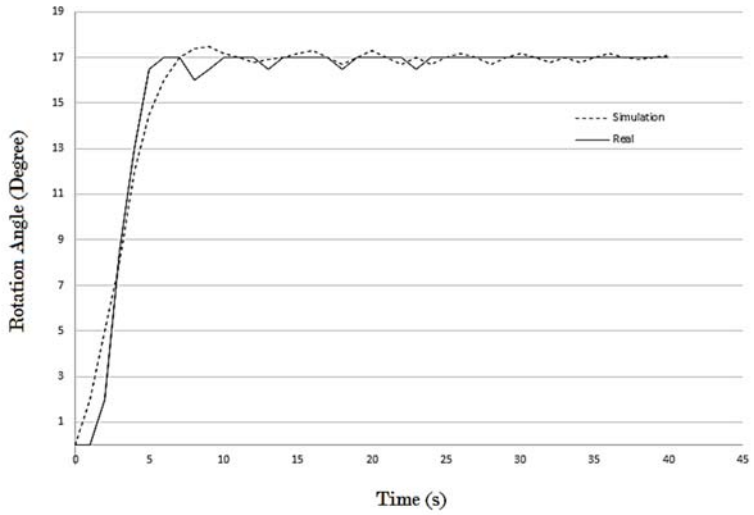

Figure 10 The rotation angle of Link 3

7 Conclusion

In this study, a new PID-fuzzy controller was designed, implemented, and tested for a constructed 3DOF prosthetic finger. To control the motion and position of the finger and also to communicate between software and hardware and to transfer the data, a driver board was designed and made for the controller. Also, the genetic algorithm was employed to optimize the gains of the designed PID controller to achieve better performance of the control system. It was seen that the GA-optimized controller has better performance than the controller trial and error.

The performance of the designed controller in achieving the desired output was tested, and the rotation of each link of the prototype robot was measured. In addition, the results of the simulation model were obtained and compared with the experimental results. The comparison of the experimental and simulation results confirms the authenticity, validity, and accuracy of the simulation model. In addition, the results showed that the output of the system has minimum overshoot and the system can reach stability over a short time and the output of the designed controller is reliable with relatively small error values. Moreover, it was shown that the prototype robot can eliminate the small vibrations which occur in the simulated robot because the prototype robot joints have friction.

References

[1] Kheirikhah, M.M., Rabiee, S., and Edalat, M.E., "A Review of Shape Memory Alloy Actuators in Robotics", David Hutchison, Lecture Notes in Computer Science, Springer-Verlag, Berlin, Vol. 6556, pp. 206-217, (2011).

[2] DeLaurentis, K.J., and Mavroidis, C., "Development of a Shape Memory Alloy Actuated Robotic Hand", Proceeding of the ACTUATOR 2000 Conference, Bremen, Germany, pp. 281-284, (2000).

[3] Kathryn, J., Laurentis, D., and Mavroidis, C., "Mechanical Design of a Shape Memory Alloy Actuated Prosthetic Hand", Technology and Health Care, Vol. 10, No. 2, pp. 91–106, (2002).

[4] Hino, T., and Maeno, T., "Development of a Miniature Robot Finger with a Variable Stiffness Mechanism using Shape Memory Alloy", International Symposium on Robotics and Automation, México, (2004).

[5] Ashrafiuon, H., Eshraghi, M., and Elahinia, M.H., "Position Control of a Three Link Shape Memory Alloy Actuated Robot", Journal of Intelligent Material Systems and Structures, Vol. 17, pp. 381-392, (2006).

[6] O'Toole, K.T., and McGrath, M.M., "Mechanical Design and Theoretical Analysis of a Four Fingered Prosthetic Hand Incorporating Embedded SMA Bundle Actuators", Proceedings of World Academy of Science Engineering and Technology, Vol. 25, pp. 142-149, (2007).

[7] Bundhoo, V., Haslam, E., Birch, B., and Park, E.J., "A Shape Memory Alloy Based Tendon-driven Actuation System for Biomimetic Artificial Fingers", Part I: Design and Evaluation, Robotica, Vol. 27, No. 1, pp. 131-146, (2009).

[8] Ahn, K.K., and Nguyen, B.K., "Position Control of Shape Memory Alloy Actuators using Self Tuning Fuzzy PID Controller", International Journal of Control, Automation and Systems, Vol. 4, pp. 756-762, (2006).

[9] Ahn, K.K., and Kha, N.B., "Modeling and Control of Shape Memory Alloy Actuators using Preisach Model Genetic Algorithm and Fuzzy Logic", Mechatronics, Vol. 18, pp. 141-152, (2008).

[10] Bizdoaca, N., Hamdan, H., and Selisteanu, D., "Fuzzy Logic Controller for a Shape Memory Alloy Tentacle Robotic Structure", Proceedings of the "IEEE Conference on Information and Communication Technologies: from Theory to Application", Damascus, Syria, pp. 1688-1693, (2006).

[11] Nicu-George, B., Anca, P., and Elvira, B., "Conventional Control and Fuzzy Control Algorithms for Shape Memory Alloy Based Tendons Robotic Structure", Wseas Trans. Systems and Control, Vol. 3, No. 2, pp. 113-124, (2008).

[12] Kheirikhah, M. M., Khodayari, A. R., and Tatlari, M., "Design a New Model for Artificial Finger by using SMA Actuators, IEEE International Conference on Robotics and Biomimetics (ROBIO2010), China, pp. 1590-1595, (2010).

[13] Kheirikhah, M. M., Khodayari, A. R., and Tatlari, M., "Design and Construction an Artificial Finger Based on SMA Actuators", Indian J. Science and Technology, Vol. 6, No. 1, pp. 3841-3848, (2013).

[14] Kaplanoglu, E., "Design of Shape Memory Alloy-based and Tendon-driven Actuated Fingers towards a Hybrid Anthropomorphic Prosthetic Hand", International Journal of Advanced Robotic Systems, Vol. 9, pp. 77-83, (2012).

[15] Gao, F., Deng, H., and Zhang, Y., "Hybrid Actuator Combining Shape Memory Alloy with DC Motor for Prosthetic Fingers", Sensors and Actuators A: Physical, Vol. 223, pp. 40–48, (2015)

[16] Lange, G., Lachmann, A., Abdul Rahim, A., Ismail, M. H., and Low, C. Y., "Shape Memory Alloys as Linear Drives in Robot Hand Actuation", Procedia Computer Science, Vol. 76, pp. 168–173, (2015).

[17] Larimi, S. R., Nejad, H. R., Hoorfar, M., and Najjaran, H., "Control of Artificial Human Finger using Wearable Device and Adaptive Network-based Fuzzy Inference System", In IEEE International Conference on Systems, Man, and Cybernetics (SMC), 003754-003758, Budapest, Hungary, (2016).

[18] Zhao, L., Ge, L., and Wang, T., "Position Control for a Two-joint Robot Finger System Driven by Pneumatic Artificial Muscles", Transactions of the Institute of Measurement and Control, Vol. 40, No. 4, pp. 1328-1339, (2018).

[19] Li, J., Zhong, G., Yin, H., He, M., Tan, Y., and Li, Z., "Position Control of a Robot Finger with Variable Stiffness Actuated by Shape Memory Alloy", In IEEE International Conference on Robotics and Automation (ICRA), pp. 4941-4946, (2017)

[20] Thoresen, A., "Artificial Finger Control-Inverse Kinematics in Soft Robotics", (Master's thesis), University of Oslo, (2019).

[21] Mirzakhani, F., Ayati, S. M., Fahimi, P., and Baghani, M., "Online Force Control of a Shape-memory-alloy-based 2 Degree-of-freedom Human Finger Via Inverse Model and Proportional–integral–derivative Compensator", Journal of Intelligent Material Systems and Structures, Vol. 30, No. 10, pp. 1538-1548, (2019).

[22] Elahania, M., and Ashrafiuon, H., "Nonlinear Control of a Shape Memory Alloy Actuated Manipulator, Trans. ASME. J. Vibe., Vol. 124, pp. 566–575, (2002).

[23] Liang, C., and Rogers, C.A., "Design of Shape Memory Alloy Actuators for Robotics, Proc. of the 4th ASME International Symposium on Robotics and Manufacturing, Santa Fe, New Mexico, Mexico, (1992).

[24] DYNALLOY data Sheet of muscle wires, DYNALLOY Inc. 14762 Bentley circle, Tustin, CA, USA, from: www.musclewires.com, (2016).

[25] Espinosa, J., Vandewalle, J., and Wertz, V., "*Fuzzy Logic, Identification and Predictive Control*, Springer-Verlag, London, (2005).

[26] Davis, L., "*Handbook of Genetic Algorithms*", VNR Comp. Library, (1990).